HYPATIA-TRACKRADAR: A SOFTWARE FOR ANIMAL TRACKING USING MARINE SURVEILLANCE RADARS

Sara Capotosti[1,2†], Martina Scacco[1,2,3†], Luca Nelli[4], Giacomo Dell'Omo[1,2] and Michele Panuccio[1,2*]

[1]*Ornis italica*, Piazza Crati 15, 00199 Rome, Italy

[2]MEDRAPTORS (Mediterranean Raptor Migration Network), c/o Michele Panuccio via Mario Fioretti 18, 00152 Rome, Italy

[3]Current affiliation: Max Planck Institute of Animal Behavior, Am Obstberg 1, 78315 Radolfzell, Germany.

[4]Institute of Biodiversity Animal Health and Comparative Medicine, University of Glasgow, Glasgow G12 8QQ, UK.

[†] These authors contributed equally to this work.

* Corresponding author: panucciomichele@gmail.com

Abstract

Hypatia-trackRadar is a Java standalone application designed to help biologists extract and process bird movement data from marine surveillance radars. This application integrates simultaneous collection of radar data and field observations by allowing the user to link information gathered from visual observers (such as bird species and flock size) to the radar echoes. A virtual transparent sheet positioned on the radar screen allows the user to visually follow and track the echoes on the radar screen. The application translates the position of the echoes on the screen in a metric coordinate system. Based on time and spatial position of the echoes the software automatically calculates multiple flight parameters, such as ground speed, track length and duration. We validated *Hypatia-trackRadar* using an unmanned aerial vehicle. Here we present the features of this application software and its first use in a real case study in a raptor migration bottle-neck.

Keywords: radar, tracking system, animal movement, Java, bird migration, drone.

1 Introduction

The movement of an animal, defined as the change in its spatial location over time, is considered a central topic in behavioural and ecological studies (Nathan et al. 2008). Bird migration is a natural event that involves the movement of a large number of individuals from breeding to wintering sites and back. An average of 2 billion birds move twice a year between Europe and Africa (Hahn et al. 2009). Interest in such impressive mass movements by the scientific community was originally driven by fascination and curiosity. Nowadays however, the study of bird movement has become an important field of research because of the mutual link between bird migration and human activities. Human activities impact the conservation of bird species and their migratory behaviour at multiple scales; in turn, current migratory patterns and their changes over time have far-reaching consequences for human societies. For this reason, monitoring and understanding bird migration has gained interest across multiple fields of research. Assessing the hazard of collision with anthropogenic infrastructures (Michev et al. 2017, Aschwanden et al. 2018), predicting the effect of climate change (Both and Marvelde 2007, Cox 2010, Saino et al. 2011, Panuccio et al. 2016a) and the spread of avian diseases (Sullivan et al. 2018, van Toor et al. 2018), and estimating seed dispersal and other ecosystem services (Kleyheeg et al. 2019) are just some examples.

Radars are widely used to investigate and monitor bird migration. The first radar studies started in 1940s and from the 1960s rapidly increased in number (Bruderer 1997a). Radars allow the remote monitoring of flying animals when visual observations are not possible, for instance during the night, at high altitudes or in case of fog. In addition, most radar systems allow simultaneous detection and tracking, at different spatial scales, of all targets moving in a certain section of the aerosphere. Over the years, different radar systems have been employed in bird migration studies. Pulse radars are particularly useful for this purpose. They use the delay between transmission and reception of the pulsed radio energy to measure the distance to a target. Examples of this system are tracking radars (derived from military equipment) and Fan-beam radars (i.e. Marine Surveillance Radars) (Cooper et al. 1991, Bruderer et al. 1995, Bruderer 1997a, 1997b). These systems, and different generations or modifications of the same system, can differ in their structure, geographical scope, data acquisition and processing, and reliability of the collected information. These differences make it challenging to compare and analyse data collected with such systems (Larkin 1991, Liechti et al. 1995, Schmaljohann et al. 2008, Stepanian et al. 2014, Dokter et al. 2011, Nilsson et al. 2018). In recent years, multiple studies have been focussing on how to calibrate different radar systems in order to collect reliable information on bird movements (Schmaljohann et al. 2008, Hilgerloh et al. 2010, Nilsson et al. 2018), and various software applications have been developed to process the different types of radar data (Dokter et al. 2011, Taylor et al. 2010, Rosa et al. 2016).

Marine Surveillance Radars have been extensively used in bird migration studies (Kerlinger and Gauthreaux 1985a, 1985b, Dokter et al. 2013, Panuccio et al. 2016b, 2019, Pastorino et al. 2017, Becciu et al. 2018). There radar systems are easy to both transport and operate and are the least expensive (Cooper et al. 1991). They use a rotating antenna to emit a narrow beam of microwaves and detect targets in their range. These radar systems are usually sold together with a software application which automatically pre-processes and transforms the radar signal of the detected targets in a two-dimensional visual output, that is directly visualised on the radar screen at each rotation of the antenna. Depending on the radar manufacturer, Marine Surveillance Radars can differ hugely in the native software they come with, but most native software display the pre-processed data using a plan position indicator (PPI). A PPI is a type of display that represents the radar location in the centre and uses concentric circles to mark the radial distance from the radar location. The radar signal is visualised on the PPI as echoes, that are a two-dimensional representation of the targets detected by the radar at each rotation of the antenna, on the horizontal or vertical plane (depending on the rotation plane of the antenna). However, the characteristics of the echoes obtained from the native radar software (in terms of number of pixels they occupy on the screen and pixel arrangement) are not directly related to the size and shape of the corresponding real target (Schmaljohann et al. 2008) and therefore cannot help the radar user in the identification of the target. Even when a pre-processing software is not involved in the procedure, the raw signal of Marine Radar systems with rotating antenna is not suitable to discriminate among species (Zaugg et al. 2008).

Researchers interested in the behavioural ecology of single species should thus integrate data obtained from this type of radar with visual observations. As early as the 1980s, Kerlinger and Gauthreaux (1985a, 1985b) combined, for the first time, the use of Marine Surveillance Radars with visual observations to study the diurnal migration of raptors in southern Texas (USA). At that time, all the equipment was analogue and the researchers used hand-held tools directly on the PPI to calculate the movements of the birds (Kerlinger and Gauthreaux 1985a, 1985b). Based on the same idea but using the currently available technology, we developed *Hypatia-trackRadar*, an open-source application software that allows the user to:

- Manually select targets on the radar screen, associate subsequent echoes of the same target to the same id and store the resulting tracks.
- Automatically calculate flight parameters related to the single echo as well as to the entire track, such as distance from the radar, track length, track straightness, ground speed) and flight altitude (for vertically oriented radars).
- Associate each track with information collected by visual observers (such as species or number of individuals).
- Standardise the collection of radar data and associated visual information to ease the comparison across studies and years.

We validated *Hypatia-trackRadar* using an unmanned aerial vehicle (UAV). The UAV was simultaneously tracked by its built-in GPS and by the radar operator (using *Hypatia-trackRadar*). For each pair of tracks, we then calculated and compared position of the centroids, length, straightness, ground speed and bearing. We finally demonstrate the use of *Hypatia-trackRadar* in a real case study, in a raptor migration bottleneck in Southern Italy.

2 Materials and Methods

2.1 Radar equipment

We used a Marine Surveillance Radar for the validation of *Hypatia-trackRadar* and its application on a real case study. The equipment consists of a 24 kW X-band radar (9.1 GHz) with a 2.17 m T-bar antenna, manufactured by the company GEM (Italy). The radar manufacturing company provides the users with the native acquisition software ExtraSea, which automatically pre-processes the raw radar signals of the detected target into a visual output (radar echoes), displayed on a PPI. The radar can be oriented horizontally or vertically, giving access to different information (Nilsson et al. 2018, Panuccio et al. 2018). For the software validation we oriented the radar horizontally, with the antenna rotating on the horizontal plane with 38 revolutions per minute (meaning that the native radar software acquires and pre-processes the radar signal into images with a 2 s interval). This radar equipment and its performances are more extensively described in Nilsson et al. (2018) and Dokter et al. (2013).

2.2 Structure of the application software

2.2.1 Programming language

Java is a general-purpose, object-oriented programming language, and it is specifically designed to have as few implementation dependencies as possible. This means that compiled Java code can run on all platforms that support Java, regardless of computer architecture and without need for recompiling (http://www.oracle.com/technetwork/java/intro-141325.html, 2/11/2015). Users commonly use a Java Runtime Environment installed on their own machines for standalone Java applications, or in a web browser for Java applets. The core of this application is composed by the Swing Framework and the java.awt.geom Package (a library of the Swing project). It provides the 2D classes for defining and performing operations on objects related to two-dimensional geometry in Java. Some important features of the package include: a) classes for manipulating geometry, such as AffineTransform and the PathIterator interface which is implemented by all Shape objects; b) classes that implement the Shape interface, such as CubicCurve2D, Ellipse2D, Line2D, Rectangle2D, and GeneralShape; c) the Area class which provides mechanisms for add (union), subtract, intersect, and exclusiveOR operations on other Shape objects. In *Hypatia-trackRadar* it was used to implement Cartesian transformations (java.awt.geom.Point2D library), and for the calculation of track metrics. Swing is a toolkit for Java, part of Oracle's Java Foundation Classes, which provides a graphical user interface (GUI) for Java programs. This toolkit allows the user to emulate the design of several platforms: in addition to familiar components such as buttons, check boxes and labels, Swing provides several advanced components such as tabbed panels, scroll panes, trees, tables, and lists. All geometric manipulations were implemented using the java.awt.geom Package.

2.2.2 Reference system

The coordinate system used by the software is centred on the radar location, corresponding to the coordinates 0,0. The position of the radar has to be set by the user before starting the data collection. The conversion factor pixel-metres allows the application to transform the XY coordinates of the echoes on the screen into a metric system, and correctly calculate all the additional parameters (such as distance of the target from the radar and flight speed). The value of this conversion factor depends on the size, in pixels, of the radar screen (specifically the diameter, in pixels, of the circle in the radar software window) and on the radar scale (range) and has to be set by the user before starting the data collection. As an example, for a radar range of 1.2 km (2400 m diameter) and a diameter on the screen of 600 pixels, the conversion factor is: 2400 *1 / 600 = 4. In this example each echo selected by the user has a minimum spatial error of ± 4 m. After setting the conversion factor, the software will associate each echo tracked by the user on the radar screen with the corresponding XY metric coordinates relative to the radar position.

2.2.3 Application modes

We implemented two different versions of the application software, one for vertically oriented and one for horizontally oriented radar antennas. Both versions of the application can deal with different flight modes (two in the current implementation, e.g. soaring and gliding/flapping). The user can manually specify, for each specific echo in a track, when a different flight mode occurs and the application will calculate the additional parameters accordingly (see section 2.2.3.1).

In the two following paragraphs we describe the additional software features and calculation of the track parameters, separately for each version.

2.2.3.1 Horizontal mode

We selected the following flight parameters to be automatically calculated on each track when the application is run in horizontal mode:

- Euclidean_distance: distance, in metres, between first and last point of each track.
- Dt: duration of the track, calculated as the difference in seconds between the time of the last point and the time of the first point of each track.
- Soaring_time: total time of soaring flight (points marked with an asterisk) for each track, in seconds. One value per track.
- Gliding_time: total time of gliding/flapping flight for each track, in seconds, calculated as the sum of the duration of gliding/flapping segments. One value per track.
- Cross_country_speed: calculated as Euclidean_distance/Dt, in km/h. One value per track.
- Track_length: total length of each track from the first to the last point, in metres, calculated as the sum of the length of all segments in a track, including soaring points. One value per track.
- Inter-thermal_length: total length of consecutive gliding/flapping segments until the next soaring segment, in metres. The occurrence of a soaring segment defines the end of a gliding/flapping bout and interrupts the calculation, thus the number of Inter-thermal_length values, separated by |, varies depending on the number of soaring segments in the track.
- Ground_speed: speed calculated separately for each gliding/flapping bout, in km/h. The number of Ground_speed values, separated by |, corresponds to the number of gliding/flapping bouts (as in the Inter-thermal_length field).
- Straightness: calculated as Euclidean_distance/Track_length. One value per track.
- Tortuosity: calculated as Track_length – Euclidean_distance. One value per track.
- Radar_distance: distance of each point from the radar centre, in metres. The number of Radar_distance values, separated by |, corresponds to the number of points in the track.

The following example shows how the application computes Track length, Inter-thermal_length and Ground_speed of a track. G1,G2,…Gn indicate gliding/flapping points of a track; S1,S2,…Sn indicate soaring points. d(G1,G2) is the distance between point G1 and point G2.

The application will interpret a selected bird track as:

G1 G2 G3 G4 S1 S2 S3 S4 G5 S5 S6

This track contains two gliding/flapping bouts, characterised by consecutive gliding/flapping segments (G1 G2 G3 G4 S1 and S4 G5 S5) and two soaring bouts (S1 S2 S3 S4 and S5 S6).

The application will calculate the track parameters as follows:

Track_length =

d(G1,G2)+d(G2,G3)+d(G3,G4)+d(G4,S1)+d(S1,S2)+d(S2,S3)+d(S3,S4)+d(S4,G5)+d(G5,S5)+d(S5,S6)

Inter-thermal_length = d(G1,G2)+d(G2,G3)+d(G3,G4)+d(G4,S1)|d(S4,G5)+d(G5,S5)

Ground_speed = v(G1 G2 G3 G4 S1) | v(S4 G5 S5)

The Inter-thermal_length is a sequence of values separated by |, each indicating the length of a gliding/flapping bout. In this example the Inter-thermal_length includes two values. The first one is the length of G1 G2 G3 G4 S1, which corresponds to the sum of the length of the segments connecting the first gliding/flapping point of the track (G1) to the first soaring point encountered along the track (S1). The second one is the length of S4 G5 S5, which corresponds to the second gliding/flapping bout. The soaring segments S1 S2 S3 S4 and S5 S6 are excluded from the calculation of the Inter-thermal_length. The Ground_speed will also have two values, corresponding to the Inter-thermal_length values divided by the temporal duration of the corresponding gliding/flapping bout.

The pseudocode of these functions is available in SM1.

2.2.3.2 Vertical mode

When *Hypatia-trackRadar* is run in vertical mode the X-axis represents the ground, in a direction that depends on the orientation of the radar, while the Y axis represents the elevation above the radar. Before starting the data collection, in addition to the radar location and the conversion factor required for both horizontal and vertical modes, the user is also required to specify the radar elevation above the sea level.

For each echo recorded in the vertical mode, the application automatically computes the elevation above the sea level and above the ground level (Fig. 1). The calculation of these two parameters depends on the initial settings provided by the user, who can:

1. Provide a terrain profile, by (a) uploading a file with comma separated values (CSV format) (recommended option for a more accurate calculation of the elevation parameters) or (b) manually drawing the profile within

the software environment.

2. Assume a flat terrain, asking the software to calculate the elevation of the echoes relative to the horizontal line passing through the radar centre.

When the first option is preferred, the file containing the terrain profile is expected to include one entry for each point of the terrain profile P(Xp,Yp). In each entry:

- Xp should correspond to the distance between P and the radar location in the direction of the radar orientation, and
- Yp should represent the elevation a.s.l. of P.

The values of both Xp and Yp are expected in metres. An example of this file is provided in the supplementary material (SM2).

Once the terrain profile is provided, the application calculates the elevation parameters as follows: given the radar centre C(xr,yr) and the terrain profile points P1(Xb1,Yb1), P2(Xb2,Yb2), ...Pn(Xbn,Ybn), the application will calculate, for each echo A (Xa,Ya), the intersection point B(Xb,Yb) between the terrain profile and the projection of the point A on the X axis (Fig. 1). The software identifies the point B(Xb,Yb) using the following algorithm:

- For each point Pi of the ground profile, it calculates the straight line passing between Pi and the next point Pi+1.
- If the line Pi-Pi+1 intersects the line passing for the input point A and parallel to the Y axis (that is, the projection of the point A on the X axis) it identifies the coordinates of the intersection point B, and it stops.
- Otherwise it continues until the next point B is found.

The application can then compute:

- Elevation above the sea level (elevation a.s.l.) = Ya + Yr.
- Elevation above the ground level (elevation a.g.l.) = elevation a.s.l. – Yb

When the user assumes a flat terrain (no terrain profile is provided) the application calculates the elevation parameters relative to a virtual line, parallel to the X-axis and passing through the radar centre:

- Elevation a.s.l. = Ya + Yr

- Elevation a.g.l. = Elevation a.s.l. – Yr

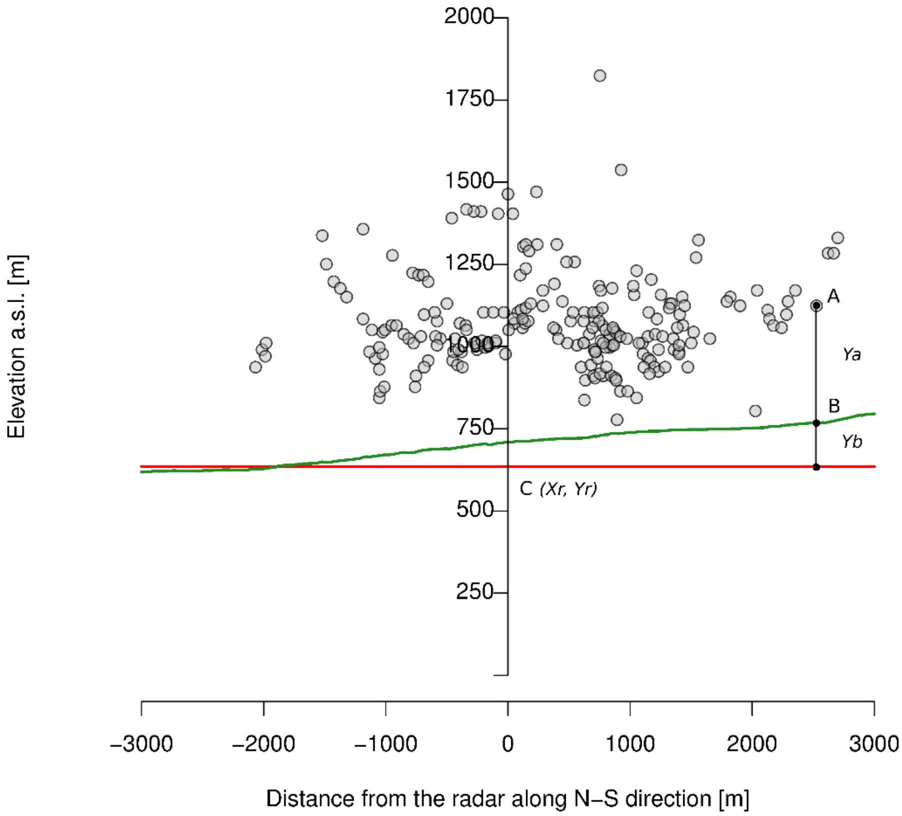

Fig. 1 - Terrain profile. Information required by *Hypatia-trackRadar* when running in vertical

mode. The origin C(Xr,Yr) represents the radar position and elevation a.s.l., used as reference for the following calculations. The line parallel to the X axis passing from the radar centre (Xr, Yr) is shown in red and the terrain profile provided by the user in green. The grey points represent the position of all radar echoes at a certain time. For each radar echo, e.g. point A, the software calculates the intersection between the projection of point A on the X axis and the terrain profile (black point B). Point B is then used by the software to compute the elevation a.g.l. (Ya in the example) and a.s.l. (Ya + Yr).

2.3 User interface and usage

When the application is run, the user is asked to select the current radar mode (horizontal or vertical). In both cases the user has to specify the position of the radar (by clicking on the screen) and the conversion factor pixels-metres. When run in vertical mode, the application additionally requires the user to specify radar elevation and terrain profile (see section 2.2.3.2). All settings required by the application at the beginning of the session can be saved by the user in the working environment. When the user restarts the application software, the last working environment is restored (anytime the user saves the working environment previous settings are overwritten). On the same machine it is possible to save simultaneously two working environments, one for the horizontal mode and one for the vertical mode. The parameters calculated by the application differ for the horizontal and the vertical mode (the mode-specific parameters have been described in section 2.2.3), whereas the user interface of the application does not change between modes.

2.3.1 Global environment

The global environment consists of two different windows: the Track Manager and the Labelling System (Fig. 2). The former includes the buttons to change the settings, open a new track, enter the track information, close and save the tracks. The latter works like a virtual transparent sheet, which can be precisely overlapped on the radar screen, by simply dragging the corners of the window. The transparency of the Labelling System allows the user to easily follow the echoes on the radar screen. The user can select the echoes of interest, by directly clicking on them on the transparent window. Each echo clicked by the user on the Labelling System is automatically stored in a CSV file with all the associated information; for safety reasons, the stored echoes are not editable from the user interface.

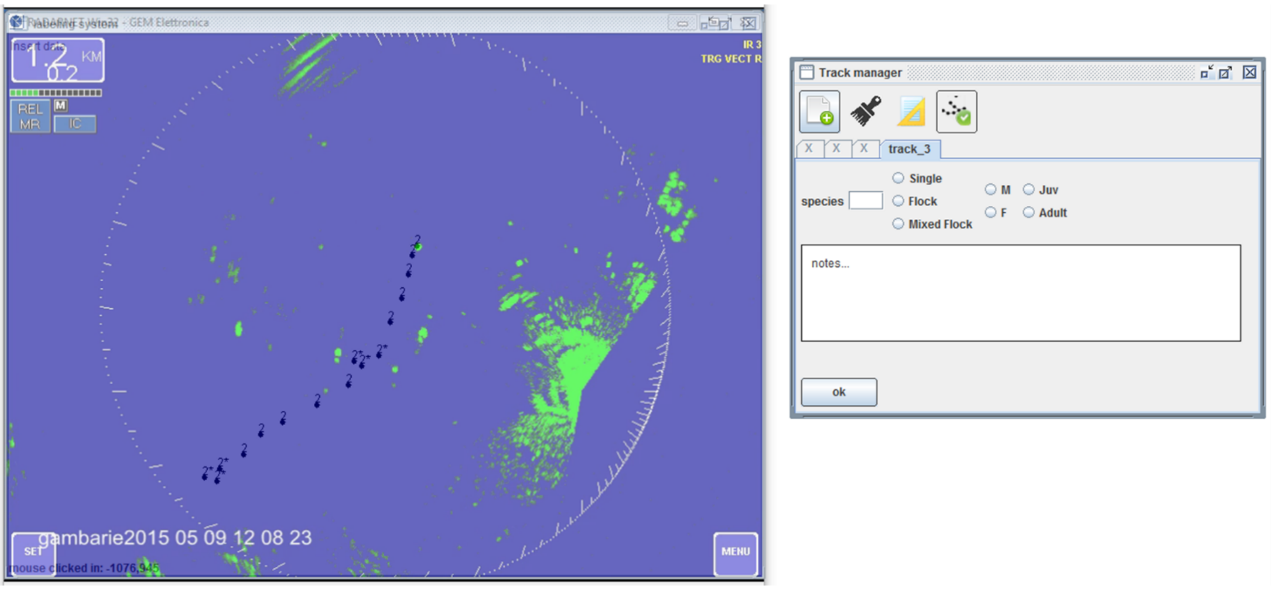

Fig. 2 - User interface. Example of the *Hypatia-trackRadar* environment. The Track Manager is focused on track 3. The id 3 is assigned to all points collected while the Track Manager window is focused on track 3, as shown in the picture. The points selected in the Labelling System are associated to the previous track, with id 2, already complete and therefore closed in the Track Manager. In the Labelling System, as well as in the final output file, an asterisk differentiates soaring points from gliding/flapping points.

When the user starts a new track in the Track Manager, each echo clicked by the user in the Labelling System is automatically associated to a unique track id, to the current timestamp (taken directly from the PC) and to metric X, Y coordinates (calculated relative to the radar centre set by the user). The sequence of all subsequent points clicked by the user will be associated to the same track id until the track is closed. More tracks can be opened simultaneously and different points can be associated to the different opened tracks by selecting them in the Track Manager window (Fig. 2). Note that once a track is closed, it cannot be reopened or edited.

2.3.2 Manually added data

In addition to the automatic information associated by the application software to each echo (track id, timestamp and XY coordinates), the Track Manager allows the user to enter, in the designated fields, additional information collected by visual observers (Fig. 2). The designated fields are:

- Flock type: S if the echo corresponds to a single individual, G for a group, MG for a mixed group (more than one species).

- Species 1.
- Species 2 (if applicable, when flock type is MG).
- Number of individuals observed in species 1.
- Number of individual observed in species 2 (if applicable, when flock type is MG).
- Sex (if applicable, when flock type is S).
- Age (if applicable, when flock type is S).
- Number of males and number of females (if applicable, when flock type is G or MG).
- Number of juveniles and number of adults (if applicable, when flock type is G or MG).
- Type of flight (set by selecting a point with the left or the right click of the mouse).
- Any additional note.

The information related to the flight mode can be acquired by the user directly from the Labelling System, by selecting a point using the left or the right button of the mouse; a right click marks the selected echoes with an asterisk (Fig. 2). This feature can be used, as in the case of this study, to separate gliding/flapping points from soaring points when tracking soaring birds. A change from gliding/flapping flight to soaring flight of a flock or a single bird can be easily detected both from the observers (when they are communicating with the radar operators) or from the radar operator (with a temporal resolution of 1 Hz, the soaring flight appears as a sequence of echoes around the same centre, with limited horizontal displacement). In addition to the automatic information associated to each echo and the manually added data, for each closed track, the application automatically calculates the parameters described in section 2.2.3, that are different depending on the application mode (horizontal or vertical) chosen at the beginning of the session.

2.3.3 Output

Any time the user closes *Hypatia-trackRadar*, a new CSV file will appear in the installation folder of the application. Each CSV file is automatically named with the application mode (horizontal or vertical) and the date and time at which the application session was started. In the file, each entry corresponds to one selected echo (point of the track); echoes belonging to the same track have different timestamp and XY coordinates but share the same track id and the same additional track information (such as group type, species, ground speed, etc).

2.4 Validation of *Hypatia-trackRadar* using an unmanned aerial vehicle

We used an unmanned aerial vehicle "DJI Phantom 3" (UAV) to validate the application software and quantify its error in the computed parameters. The UAV was simultaneously tracked by its built-in GPS and by *Hypatia-trackRadar* using a Marine Surveillance Radar (see section 2.1 for details on the radar equipment). The radar was operated at 2 km range, which given the setup of the native software window, implied a conversion factor of 6.67 (1 px = 6.67 m). We used a double-blind approach, in which the radar operator was isolated from the aerial vehicle sight. We flew the UAV along 46 flight tracks, under different scenarios of speed, straightness, and bearing, which are among the most common flight parameters recorded during studies on bird movement (Spaar 1997, Meyer et al. 2000, Malmiga et al. 2014, Nilsson et al. 2018). Each flight was simultaneously tracked by the radar operator (using *Hypatia-trackRadar*) and recorded by the built-in GPS of the UAV (135 Hz temporal resolution). We assumed the GPS provided precise and accurate information, and therefore used the GPS tracks as a reference to validate the radar tracks. For each track recorded by the radar we considered the following parameters: Track_length, Ground_speed, Cross_country_speed, tortuosity (all automatically calculated by the application *Hypatia-trackRadar*), flight direction and centroid of the track on the XY plane (both calculated in R during the data analysis (R Core Team 2018)); flight direction was calculated as the angle, in clockwise degrees from the North, of the straight line connecting the first and the last point of the track). The same flight parameters were calculated for the tracks collected by the GPS of the UAV, using the same procedure implemented by *Hypatia-trackRadar* for all variables except the ground speed, as we considered the instantaneous ground speed provided by the built-in GPS as more accurate. We then compared the distribution of the flight parameters of tracks collected with the two methods using a non-parametric test for paired samples (Wilcoxon test). To compare flight directions we used a Watson-Wheeler test for circular paired samples using the R package "circular" (Agostinelli and Lund 2017). For the ground speed and the centroids of the tracks, we additionally investigated if the flight parameters of the UAV could partially explain the difference in the parameters calculated with the two tracking methods. Specifically, we used the difference in ground speed (Δ ground speed = $\text{Hypatia}_{\text{speed}}$ - $\text{GPS}_{\text{speed}}$), the difference in tortuosity (M2; Δtortuosity = $\text{Hypatia}_{\text{tortuosity}}$ – $\text{GPS}_{\text{tortuosity}}$) and the distance between the centroids of the tracks collected with the two methods as response variables in three separate linear regression models. We used the distance between centroids as a measure of distortion in the track recorded by the radar. The following parameters (measured by the built-in GPS of the UAV) were used as explanatory variables: ground speed (m/s), radial distance from the radar (m), vertical distance from the horizontal plane of the radar (difference in the elevation between the UAV and the radar in m), maximum change in elevation within the track (calculated as the difference between the minimum and the maximum elevation of the GPS track) (m), and track tortuosity (m). The response variable "distance between centroids" was log-transformed to match the model assumptions. All analyses were performed in R (R Core Team 2018).

2.5 Application of *Hypatia-trackRadar* to track migrating birds

We used *Hypatia-trackRadar* for the first time at the Strait of Messina (southern Italy), a well-known bottleneck for migrating raptors in the Mediterranean basin (Panuccio 2011). We used *Hypatia-trackRadar* with the radar equipment described in section 2.1 to collect data on bird movement during Spring and Autumn migration, in 2015. During both Spring and Autumn, the radar was operated horizontally, at a 2 km scale (same settings as for the validation with the UAV). The radar station was located at 15.799501° long, 38.230814° lat in Spring and at 15.823741° long, 38.215285° lat in Autumn.

3 RESULTS

3.1 Validation of *Hypatia-trackRadar* using an unmanned aerial vehicle

The considered flight parameters, calculated with *Hypatia-trackRadar* and with the built-in GPS of the UAV, showed overall similar results. However, the distribution of the ground speed and track straightness recorded with the two methods showed significant differences.

Table 1. Result of test for paired samples of different flight parameters for tracks collected with the two methods. The value W indicates the results of non-parametric Wilcoxon test, or in the case of Bearing, Watson-Wheeler test. We also show the mean and standard error of the difference between the same parameters of the two methods.

Flight parameter	Difference *Hypatia* – GPS	Test for paired samples

	(mean ± st.err.)	(W, p-value)
Track length (m)	17.868 ± 4.99	1100, 0.747
Tortuosity (m)	25.760 ± 2.791	1361, 0.018
Ground speed (m/s)	0.897 ± 0.226	1061, 0.055
Cross country speed (m/s)	0.474 ± 0.219	894, 0.699
Distance between centroids (m)	28.889 ± 3.567	Centroid coord X: 1075, 0.898 Centroid coord Y: 1061, 0.985
Bearing (°)	0.347 ± 0.003	0.007, 0.996

Specifically, the ground speed estimated by *Hypatia-trackRadar* (mean ± SE = 13.39 ± 0.27 m/s), was just under 1 m/s higher than the one measured by the GPS (12.66 ± 0.28), whereas the average track tortuosity measured by *Hypatia-trackRadar* (76.26 ± 12.47), was about 26 m higher than the one derived from the GPS (48.53 ± 10.95; Table 1). The distribution of the track centroids (calculated for X and Y coordinates separately; Table 1) did not significantly differ between the two methods, but some distortion can be visually detected in Fig. 3.

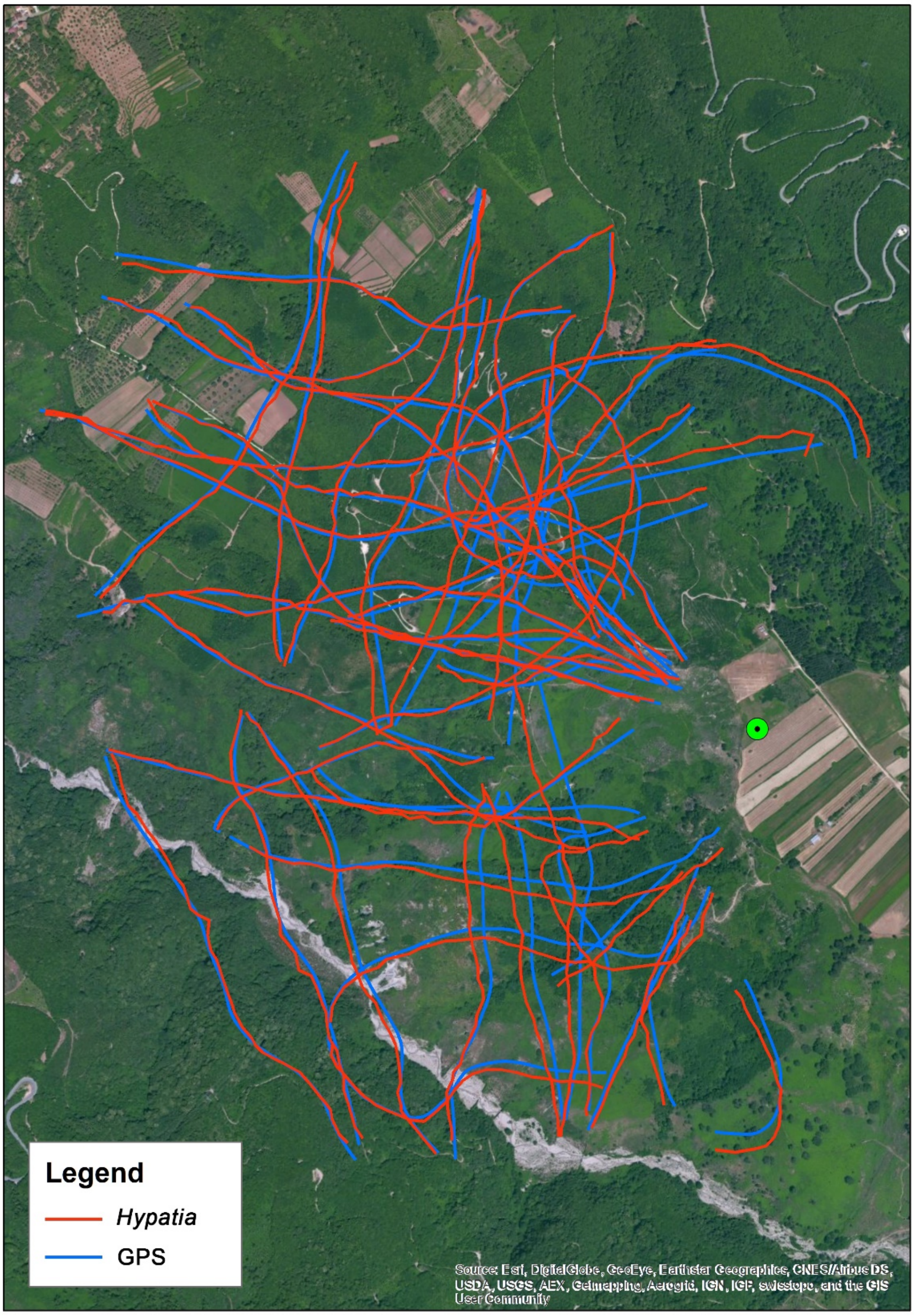

Fig. 3 – Tracks of the UAV. Visualization of the tracks of the UAV collected with *Hypatia-trackRadar* (in red) and the built-in GPS of the UAV (in blue). The green point indicates the radar location.

We used three linear models to investigate if the difference in speed and tortuosity, and the distance between the centroids of the tracks recorded with the two methods could be affected by the flight parameters of the target (the UAV) (Table 2; section 2.4).

Table 2. Summary of the three linear models. All predictors were measured by the built-in GPS of the UAV. Results show estimates and standard errors.

	Response variables: Δ ground speed (*Hypatia* - GPS)	Δ tortuosity (*Hypatia* - GPS)	log(distance between centroids)
Intercept	4.902^{***}	37.147	3.147^{***}
	(1.765)	(25.419)	(1.020)
Ground speed	-0.357^{***}	-1.168	0.037
	(0.129)	(1.854)	(0.074)
Radial distance from Radar	0.0004	-0.003	-0.001^{*}
	(0.001)	(0.013)	(0.001)
Tortuosity	0.003	0.100^{**}	-0.003^{*}
	(0.003)	(0.047)	(0.002)
Change in elevation within track	0.007	0.110	-0.001
	(0.009)	(0.132)	(0.005)
Vertical distance from radar horizontal plane	-0.004	0.020	0.013^{**}
	(0.011)	(0.160)	(0.006)
Observations	37	37	37
R^2	0.236	0.176	0.246
Adjusted R^2	0.113	0.043	0.124
Note:	*p<0.1; **p<0.05; ***p<0.01		

The results of the linear models showed that the difference between the ground speed recorded with the two methods decreased with increasing speed of the UAV (estimate ± SE = -0.357 ± 0.128, P<0.01), whereas the difference in tortuosity significantly increased with increasing track tortuosity of the UAV (0.100 ± 0.047,

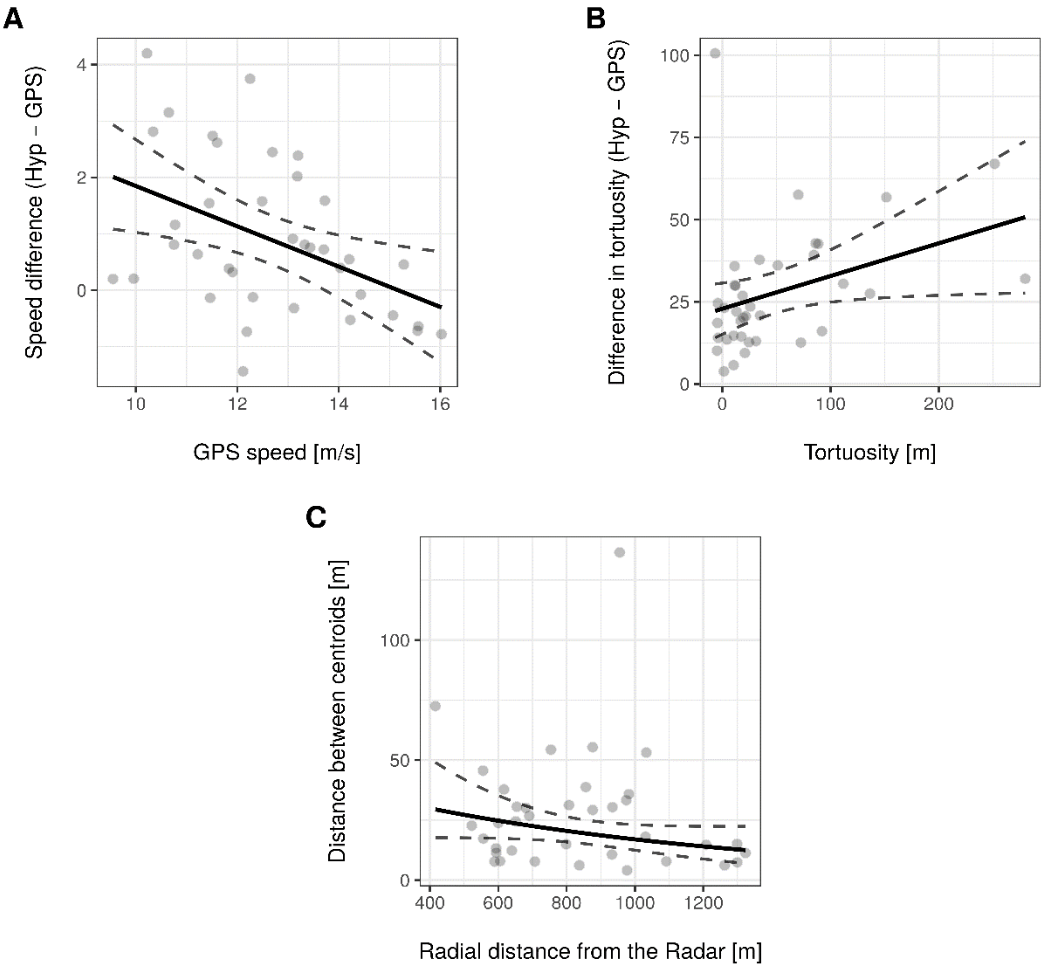

p<0.05; Table 2; Fig. 4a, 4b). The distance between centroids was affected by multiple parameters; specifically, the model showed a significant increase of about 1.3% with one unit increase in vertical distance from the radar (above or below the radar horizontal plane), a decrease of 1% with one unit increase in radial distance from the radar and a decrease of 3% with one unit increase in tortuosity (Table 2; Fig. 4c). These results indicate that higher ground speed of the target and lower tortuosity in its flight, the higher the accuracy of the flight parameters recorded by the radar. They also show that tracks with higher tortuosity, recorded closer to the radar horizontal plane and farther away from its location are more accurately positioned relative to the GPS tracks.

Fig. 4 – Result of the linear models. Partial effect plots for the three linear regression models, investigating the relationship between the flight parameters of the UAV and the difference in the measurements of *Hypatia-trackRadar* and the built-in GPS. Specifically, the three plots show the effect of the speed (A), tortuosity (B) and radial distance (C) of the UAV on the difference in speed, tortuosity and distance between centroids, respectively. In all plots, the solid points correspond to the observations used in the models; the solid lines represent the regression lines and the dashed lines the 95% confidence intervals.

3.2 Application of *Hypatia-trackRadar* to track migrating birds

During Spring and Autumn migration in 2015, we used *Hypatia-trackRadar* to collect about 1000 tracks of migrating raptors and storks. The output of *Hypatia-trackRadar* corresponding to a selection of these tracks with the

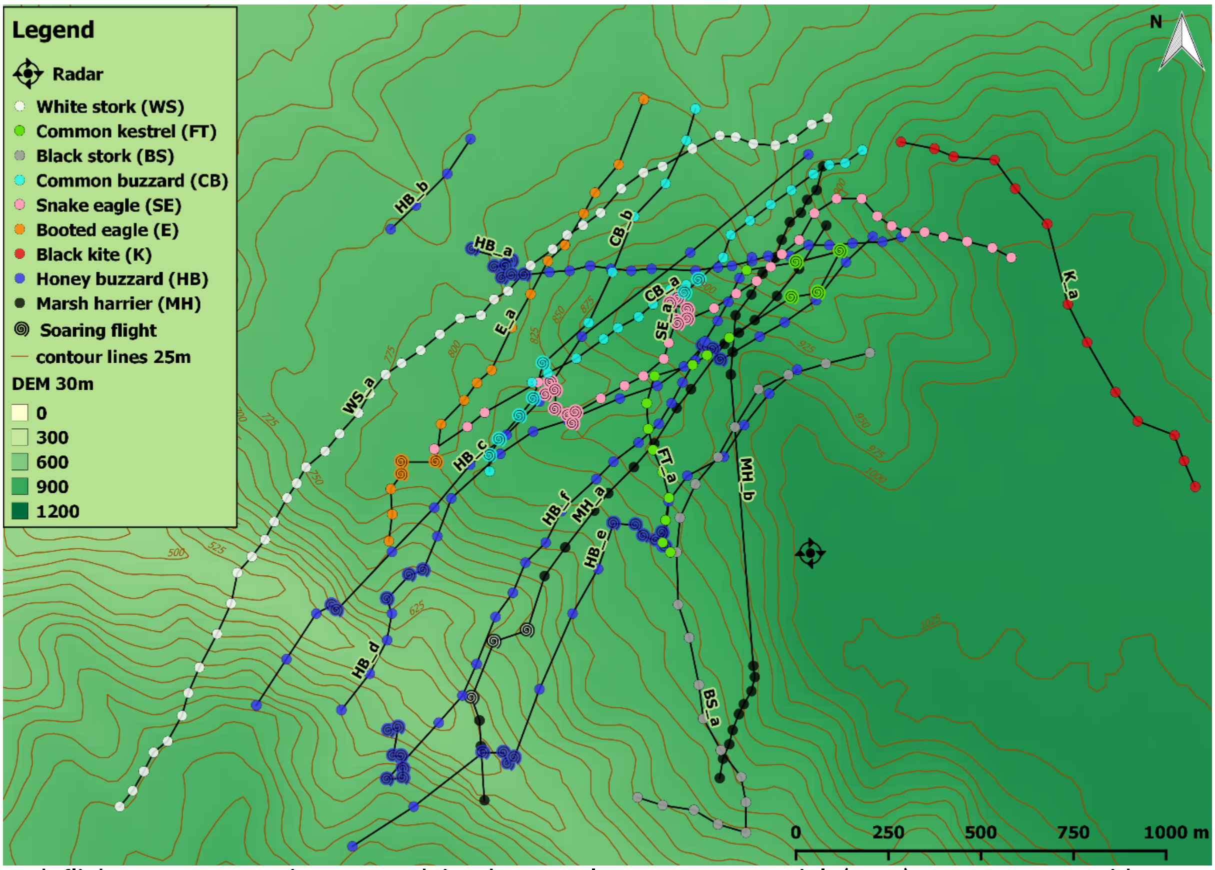

associated flight parameters is reported in the supplementary material (SM3). Here we provide two visualizations of the application output, separate for the two migratory seasons, with tracks of individuals from different species performing both gliding/flapping flight and soaring flight (Fig. 5).

A

B

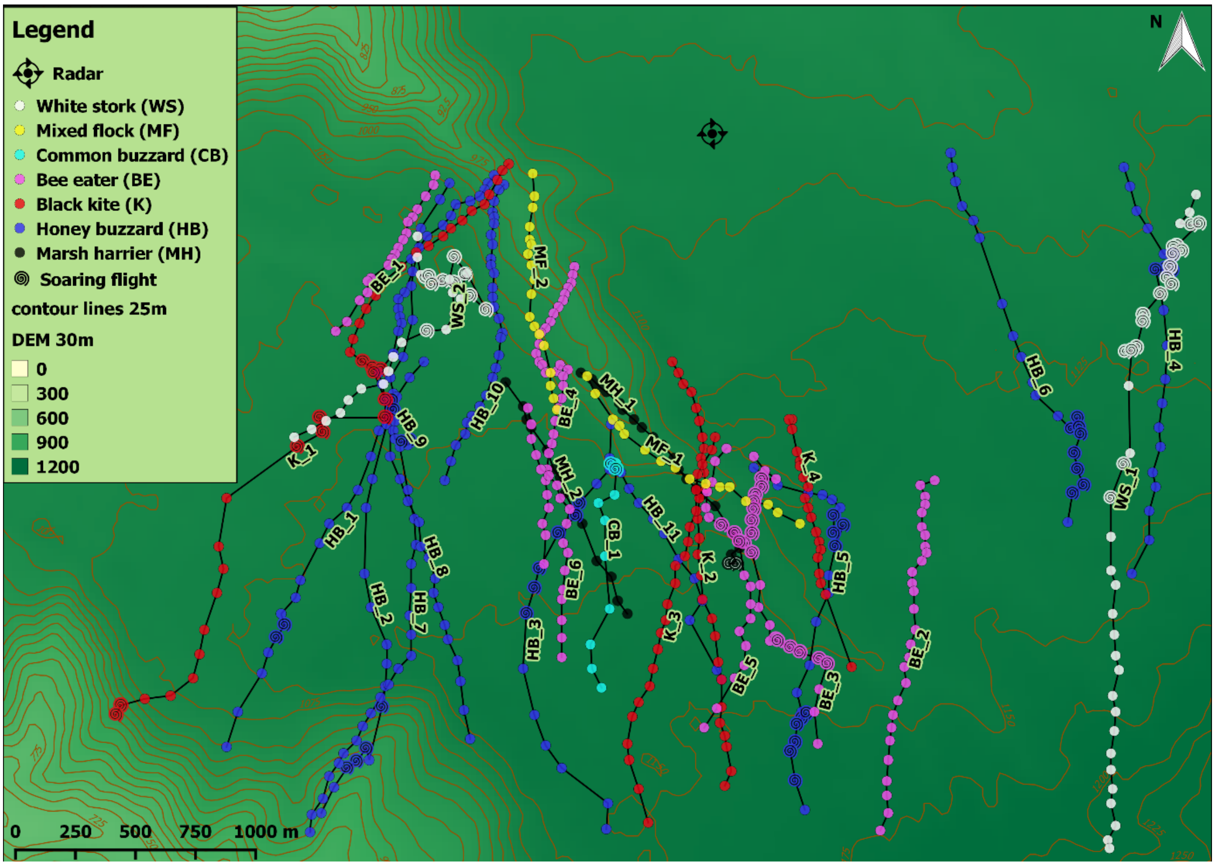

Fig. 5 – Tracks of migrating birds. Selection of tracks collected at the Strait of Messina using *Hypatia-trackRadar* and a Marine Surveillance Radar, in Spring (A) and Autumn (B) 2015. Different colours indicate different bird species. Solid points correspond to gliding/flapping

flight and spiral points to soaring flight. Background colour and contour lines are based on a 30 m resolution Digital Elevation Model (DEM) (EEA 2013). The map was prepared using the open source GIS software QGIS (QGIS Development Team 2017). The flight parameters automatically associated by *Hypatia-trackRadar* to each track are presented in the supplementary material (SM3).

DISCUSSION

The use of the UAV, and the assumed accuracy of the information collected by the built-in GPS, allowed us to test the reliability of the information provided by *Hypatia-trackRadar*. The results showed a general agreement between the flight parameters and the position of the tracks collected by the GPS and by *Hypatia-trackRadar*. However, we detected some differences in the ground speed, track tortuosity and track centroids. In the explanation of the fine scale differences detected during the validation, three main sources of bias have to be taken into account, related to hardware, software and user. First, the intrinsic error of the GPS (the positioning system of the UAV) and the radar equipment (the tool used to detect the target). Second, the error in the native radar software used to transform the radar signal into a visual output on the screen (the target is represented by a green echo on the screen, whose size in pixels is not directly related to the real size of the target), and the error of *Hypatia-trackRadar*. Finally, the precision of the radar operator selecting the radar echoes on the screen. The error of *Hypatia-trackRadar* mainly depends on the scale at which the radar is used, which is directly related to the pixel-metres conversion of each measurement (in our study case at 2 km scale, 1 pixel=6.67 m). This conversion factor in turn affects the impact of the manual error potentially made by the user while selecting echoes on the screen. Additionally, the echo visualised on the screen can occupy multiple neighboring pixels. For these reasons, the biases introduced by the *Hypatia-trackRadar* application and by the radar operator are expected to play a minor role when the radar is used at a scale < 2 km and a bigger role when the radar is used at larger scales. Our validation showed that all parameters collected with the combination of radar equipment, *Hypatia-trackRadar* and radar operator were overestimated relative to the ones collected with the built-in GPS of the UAV, but the differences between the two methods are small and mostly non-significant. Our models suggest that all sources of biases might be contributing to the differences detected in our dataset. In fact, our results show that lower ground speed and higher tortuosity in the flight of the target lead to higher differences in the flight parameters collected with the two methods. Specifically, a target flying both at a low (about 10 m/s) and a high (16 m/s) ground speed would lead to a higher difference in the ground speed calculated with the two methods. Assuming the GPS measurement is more accurate, a lower ground speed of the target leads to an overestimation of the speed calculated with the radar system, whereas a higher ground speed leads to an underestimation. We suggest that the proximate cause of this bias is the imprecision of the radar operator while selecting the targets on the screen. A slow flying target is more unpredictable in its flying direction leading to errors perpendicular to the flying direction. In contrast, a fast flying target can make it difficult for the radar operator to keep up with its track leading to errors along the direction of the track. The extent of the error in the recorded ground speed is closely related to the scale at which the radar operates (defining how many meters of error will be produced when the user commits an error of one pixel). Concerning the Δtortuosity, a minimum value of tortuosity (straighter tracks) in the UAV flight seemed to minimise this difference. Finally, the last model showed how tracks of targets flying slower, closer to the horizontal plane of the radar (low vertical distance), farther away from the radar (high radial distance) and with less change in altitude within the track, are less subject to distortions. This result is in agreement with our expectation concerning the results of the previous models and the distortion caused by the radar equipment, mainly due to the ground clutter (close to the radar) and to the shape and the width of the radar beam (the latter increases with the distance from the radar); these effects are also visually detectable in Fig. 3. Unexpectedly, this model also showed that an increased tortuosity would decrease the distance between centroids, but we did not find a possible direct cause for this result. Overall, considering the different sources of bias involved in the calculation and comparison of the flight parameters collected with the two methods, this validation showed that the distortions detected in the tracks recorded by the radar occur at very fine scale. The validation also highlighted the effect of the different factors and sources of bias affecting these distortions and can be used as a reference during the analysis and interpretation of radar data.

After the Marine Surveillance Radar and the native radar software are correctly calibrated, *Hypatia-trackRadar* allows the user to collect and store standardised data on the spatial displacement of animals moving in the radar range, and to integrate these data with information collected through visual observation regarding species, flock size, sex and flight behaviour of the tracked individuals. Beyond the need of these additional information per se, they also help the radar operator to minimise the misinterpretation of the radar echoes appearing on the screen, reducing one of the main biases in avian studies involving the use of radar systems (Larkin 1991, Schmaljohann et al. 2008). *Hypatia-trackRadar* can be used on any type of radar system that allows visualisation of echoes on a PPI on a personal computer (for an example of this application used with a broad-band radar see Xirouchakis and Panuccio 2019). The user interface of the application is flexible and can be adapted to the screen of different native radar software (which are different according to the manufacturing company selling the radar equipment). The output files of *Hypatia-trackRadar* can be directly used for the analysis of the flight parameters that are automatically calculated by the application. In addition, the metric coordinates assigned to each echo relative to the radar position allow the users to easily calculate additional movement parameters, localise the data in a geographic reference system, visualise them in their environmental context, and associate them to environmental information.

In conclusion, the availability of a simple and flexible software application as *Hypatia-trackRadar* is promising for meeting the needs of different radar studies, by easing the acquisition, standardisation and analysis of radar data associated with observational data of flying animals.

Hypatia-trackRadar is an open source application, freely-available at: http://www.radar4birds.com/hypatia-trackradar/

Acknowledgements

This research was supported by TERNA Rete Italia S.p.A. Additional support for the fieldwork was given by *Ornis italica* and MEDRAPTORS (Mediterranean Raptor Migration Network). M.P. was partially financed through a grant from Crowdfunding Platform 'Universitiamo' of the University of Pavia for the project 'Wings Over the Straits' and by *Ornis italica*. We acknowledge the support provided by COST—European Cooperation in Science and Technology through the Action ES1305 "European Network for the Radar Surveillance of Animal Movement" (ENRAM). The authors would like to thank Nora Carlson and two anonymous reviewers for their constructive feedback on the manuscript.

References

Agostinelli C. and Lund U. 2017. R package 'circular': Circular Statistics (version 0.4-93). https://r-forge.r-project.org/projects/circular/.

Aschwanden J., Stark H., Peter D., Steuri T. and Liechti F. 2018. Bird collisions at wind turbines in a mountainous area related to bird movement intensities measured by radar. Biological Conservation 220: 228-236.

Becciu P., Panuccio M., Catoni C., Dell'Omo G. and Sapir N. 2018. Contrasting effects of tailwind and asymmetrical response to crosswinds in soaring migrants. Behavioral Ecology and Sociobiology 72: 28.

Both C. and Marvelde L.T. 2007. Climate change and timing of avian breeding and migration throughout Europe. Climate Research 35: 93–105.

Brown D.D., Kays R., Wikelski M., Wilson R. and Klimely A.P. 2013. Observing the unwatchable through acceleration logging of animal behavior. Animal Biotelemetry 1: 20.

Bruderer B. 1997a. The study of migration by radar. Part 1: the technical basis. Naturwissenschaften 84:1-8.

Bruderer B. 1997b. The study of migration by radar. Part 2: major achievements. Naturwissenschaften 84: 45-54.

Bruderer B., Steuri T. and Baumgartner M. 1995. Short-range high-precision surveillance of nocturnal migration and tracking of single targets. Israel Journal of Zoology 41: 207–220.

Cooper B.A., Day R.H., Ritchie R.J. and Cranor C.L. 1991. An improved marine radar system for studies of bird migration. Journal of Field Ornithology 62: 367–377.

Cox G.W. 2010. Bird Migration and Global Change. Washington DC: Island Press.

Dokter A.M., Baptist M.J., Ens B.J., Krijgsveld K.L. and van Loon E. 2013. Bird radar validation in the field by time-referencing line-transect survey. PloS One 8: e74129.

Dokter A.M., Liechti F., Stark H., Delobbe L., Tabary P. and Holleman I. 2011. Bird migration flight altitudes studied by a network of operational weather radars. Journal of Royal Society Interface 8: 30-43.

EEA 2013. European Environment Agency - Digital Elevation Model over Europe (EU-DEM). https://www.eea.europa.eu/data-and-maps/data/eu-dem.

Hahn S., Bauer S. and Liechti F. 2009. The natural link between Europe and Africa - 2.1 billion birds on migration. Oikos 118: 624-626.

Hilgerloh G., Caprano T. and Griebeler E.M. 2010. Calibrating the operational beam width and maximum range of a ship radar used for bird observations. The Journal of Navigation 63: 363-371.

Kerlinger P. and Gauthreaux S. 1985a. Seasonal timing, geographic distribution, and flight behavior of Broad-winged Hawks during spring migration in South Texas: a radar and direct visual study. Auk 102: 735–743.

Kerlinger P. and Gauthreaux S. 1985b. Flight behavior of raptors during spring migration in South Texas studied with radar and visual observations. Journal of Field Ornithology 56(4): 394–402.

Kleyheeg E., Fiedler W., Safi K., Waldenström J., Wikelski M. and van Toor M.L. 2019. A Comprehensive Model for the Quantitative Estimation of Seed Dispersal by Migratory Mallards. Frontiers in Ecology and Evolution 7: 40.

Larkin R. 1991. Flight speeds observed with radar, a correction: slow 'birds' are insects. Behavioural Ecology Sociobiology 29: 221–224.

Liechti F., Bruderer B. and Paproth H. 1995. Quantification of nocturnal bird migration by moonwatching: comparison with radar and infrared observations. Journal of Field Ornithology 66: 457–468.

Malmiga G., Nilsson C., Bäckman J. and Alerstam T. 2014. Interspecific comparison of the flight performance between sparrowhawks and common buzzards migrating at the Falsterbo peninsula: A radar study. Current Zoology 60: 670–679.

Meyer S.K., Spaar R. and Bruderer B. 2000. To cross the sea or to follow the coast? Flight directions and behavior of migrating raptors approaching the Mediterranean Sea in autumn. Behavior 137: 379–399.

Michev B., Zehtindjiev P., Marinov M.P. and Liechti F. 2017. Relationship between the intensity of nocturnal migration measured by radar and the anthropogenic mortality of birds. Acta Zoologica Bulgarica 69: 229-237.

Nathan R., Getz W.M., Revilla E., Holyoak M., Kadmon R., Saltz D. and Smouse P.E. 2008. A movement ecology paradigm for unifying organismal movement research. 105: 19052-19059. https://doi.org/10.1073/pnas.0800375105

Nilsson C., Dokter A., Schmid B., Scacco M., Verlinden L., Bäckman J., Haase G., Dell'Omo G., Chapman J., Leijnse H. and Liechti F. 2018. Field validation of radar systems for monitoring bird migration. Journal of Applied Ecology 55: 2552-2564.

Panuccio M. 2011. Wind effects on visible raptor migration in spring at the Strait of Messina, Southern Italy.

Journal of Raptor Research 45: 88-92.

Panuccio M., Dell'Omo G., Bogliani G., Catoni C. and Sapir N. 2019. Migrating birds avoid flying through fog and low clouds. International Journal of Biometeorology 63: 231-239.

Panuccio M., Martin B., Morganti M., Onrubia A. and Ferrer M. 2016a. Long-term changes in autumn migration dates at the Strait of Gibraltar reflect population trends of soaring birds. Ibis 159: 55-65.

Panuccio M., Stanzione V., Catoni C., Santini M. and Dell'Omo G. 2016b. Radar tracking reveals influence of crosswinds and topography on migratory behavior of European honey buzzards. Journal of Ethology 34: 73-77.

Panuccio M., Agostini N., Bogliani G. and Dell'Omo G. 2018. Migrating raptor counts: the need for sharing objectives and field protocols, and the benefits in using a radar. Bird Study 65: S77-S84.

Pastorino A., Ramirez Roman J., Agostini N., Dell'Omo G. and Panuccio M. 2017. Fog and rain lead migrating White storks *Ciconia ciconia* to perform reverse migration and to land. Avocetta 41: 5-12. https://doi.org/10.30456/AVO.2017102

QGIS Development Team 2017. QGIS Geographic Information System. Open Source Geospatial Foundation Project. http://qgis.osgeo.org.

R Core Team 2018. R: A language and environment for statistical computing. R Foundation for Statistical Computing, Vienna, Austria. ISBN 3-900051-07-0.

Rosa I.M.D., Marwues A.T., Palminha G., Costa H., Mascarenhas M., Fonseca C. and Bernardino J. 2016. Classification success of six machine learning algorithms in radar ornithology. Ibis 158: 28-42.

Saino N., Ambrosini R., Rubolini D., Von Hardenberg J., Provenzale A., Huppop K., Huppop O., Lehikoinen A., Lehikoinen E., Rainio K., Romano M. and Sokolov L. 2011. Climate warming, ecological mismatch at arrival and population decline in migratory birds. Proc. R. Soc. B 278: 835–842.

Schmaljohann H., Liechti F., Bächler E., Steuri T. and Bruderer B. 2008. Quantification of bird migration by radar – a detection probability problem. Ibis 150: 342-355.

Spaar R. 1997. Flight strategies of migrating raptors. A comparative study of interspecific variation in flight characteristics. Ibis 139: 523–535.

Stepanian P.M., Chilson P.B. and Kelly J.F. 2014. An introduction to radar image processing in ecology.

Methods in Ecology and Evolution 5: 730-738.

Sullivan J.D., Takekawa J.Y., Spragens K.A., Newman Scott .H., Xiao X., Leader P.J., Smith B. and Prosser D.J. 2018. Waterfowl spring migratory behavior and avian influenza transmission risk in the changing landscape of the east asian-australasian flyway. Frontiers in Ecology and Evolution 6: 206.

Taylor P.D., Brzustowski J.M., Matkovich C., Peckford M.L. and Wilson D. 2010. radR: an open-source platform for acquiring and analysing data on biological targets observed by surveillance radar. BMC Ecology 10: 22.

van Toor M.L., Avril A., Wu G., Holan S.H. and Waldenström J. 2018. As the duck flies - Estimating the dispersal of low-pathogenic avian influenza viruses by migrating mallards. Frontiers in Ecology and Evolution 6: 208.

Xirouchakis S. and Panuccio M. 2019. Hunting altitude of Eleonora's falcon (*Falcon eleonorae*) over a breeding colony. Journal of Raptor Research 53: 56-65.

Zaugg S., Saporta G., van Loon E., Schmaljohann H. and Liechti F. 2008. Automatic identification of bird targets with radar via patterns produced by wing flapping. Journal of Royal Society Interface 5: 1041-1053.

SM1. Pseudocode of the parameters computed by *Hypatia-trackRadar*, in horizontal and vertical mode.

1) <u>For the parameters calculated in horizontal mode:</u>

```
for(Point nextPoint :listPoint):

	Soaring = false;
	firstTrackLengthX = secondTrackLengthX;
	firstTrackLengthY = secondTrackLengthY;
	if(!hasFirstTimeTrackLength){
		firstTimeTrackLength = timeTrackLength;
		timeTrackLength = nextPoint.hour;
		hasFirstTimeTrackLength = true;
	}
	if(nextPoint.fliType.equals("*")){
		IS A SOARING POINT
		Soaring = true;
	}else{Soaring = false;}

	if(!hasFirstPoint){
		firstX = nextPoint.x;
		firstY = nextPoint.y;
		starTime = nextPoint.h;
		hasFirstPoint = true;
```

```
        last_index = nextPoint.index;
}
if(checkPoint){
        if(Soaring){isFirstSoaring=true;}else{isFirstSoaring=false;}
}
if(lastIndex = nextPoint.index){
        IS A POINT OF THE CURRENT TRACK

        Radardistance = distance(0, 0, x, y);
        if(Radardistance >0){
        radarDistanceString += radarDistance +"|"; }
        secondTrackLengthX = nextPoint.x;
        secondTrackLengthY = nextPoint.y;
        endTimeTrackLength = nextPoint.h;
        if(!Soaring && !start){
        distance = distance(firstTrackLengthX, firstTrackLengthY, secondTrackLengthX,
                secondTrackLengthY);
        trackLengthWithSoaring = trackLengthWithSoaring + distance;
        isFirstSoaring = true;

        }else{

        CASE 1: TRACK MORPHOLOGY IS G1G2G3S1S2S3

        distance = distance(firstTrackLengthX, firstTrackLengthY, secondTrackLengthX,
```

```
secondTrackLengthY);
trackLengthWithSoaring = trackLengthWithSoaring + distance;
if( trackLengthWithSoaring > 0){
    trackLengthWithSoaringString += trackLengthWithSoaring + "|";
```

GROUND SPEED CALCULATION:

TAKE TIME OF THE START AND THE END POINT TRACK

```
if(firstTimeTrackLength!=null){
    time_1 = (firstTimeTrackLength);
}else{
if(timeTrackLength!=null){
time_1 = (timeTrackLength);}

if(endTimeTrackLength!=null){
time_2 = (endTimeTrackLength);}

diff = 0;
diffSeconds = 0;

if(time_1!=null && time_2!=null ){
diff = time_2 - time_1;
diffSeconds = diff / 1000;
gliding_time = gliding_time + diffSeconds;
```

```
}



Km_trackLengthWithSoaring =  trackLengthWithSoaring * 0.001;
ground_speed = 0;
hour = (diffSeconds / 3600.0);

if(hour>0){
        ground_speed = Km_trackLengthWithSoaring/hour;
}
ground_speedString += ground_speed +"|";
trackLengthWithSoaring = 0;
hasFirstTimeTrackLength = false;

}
isFirstSoaring = true;
```

CASE 2: TRACK MORPHOLOGY IS S1ABCDE

```
distance = distance(firstTrackLengthX, firstTrackLengthY, secondTrackLengthX,
        secondTrackLengthY);
trackLengthWithSoaring = trackLengthWithSoaring + distance;
if( trackLengthWithSoaring > 0){
trackLengthWithSoaring_string += trackLengthWithSoaring + "|";
```

GROUND SPEED CALCULATION:

TAKE TIME OF THE START AND THE END POINT OF THE TRACK

```
if(firstTimeTrackLength!=null){
	time_1 = (firstTimeTrackLength);
}else{
if(timeTrackLength!=null){
	time_1 = (timeTrackLength);}

if(endTimeTrackLength!=null){
	time_2 = (endTimeTrackLength);}

diff = 0;
diffSeconds = 0;

if(time_1!=null && time_2!=null ){
	diff = time_2 - time_1;
	diffSeconds = diff / 1000;
	gliding_time = gliding_time + diffSeconds;
}

Km_trackLengthWithSoaring =  trackLengthWithSoaring * 0.001;
ground_speed = 0;
```

```
hour = (diffSeconds / 3600.0);



if(hour>0){
        ground_speed = Km_trackLengthWithSoaring/hour;
}
ground_speedString += ground_speed +"|";
trackLengthWithSoaring = 0;
hasFirstTimeTrackLength = false;

}
isFirstSoaring = true;
isFirstSoaring = true;
}
CASE 3: TRACK MORPHOLOGY IS S1S2S3
hasFirstTimeTrackLength = false;
}

if(!start){
CALCULATE NORMAL TRACKLENGTH

distance = distance(firstTrackLengthX, firstTrackLengthY, secondTrackLengthX,
        secondTrackLengthY);
trackLength = trackLength+distance;
}
```

```
        checkPoint = false;
}}
if(lastIndex != nextPoint.index){
START A NEW TRACK

if(Soaring){isFirstSoaring=true;}else{isFirstSoaring=false;}



DT CALCULATION FOR THE LAST TRACK:

time1 = starTime;
time2 = endTime;
diff = time2 - time1;
diffSeconds = diff / 1000;

CROSS-COUNTRY SPEED CALCULATION FOR THE LAST TRACK:

cross_country_speed = 0;
km_LinearDistance = linear_distance * 0.001;
hour = (diffSeconds / 3600.0);

if(hour > 0){
        cross_country_speed = km_LinearDistance/hour;
}
```

GROUND SPEED CALCULATION FOR THE LAST TRACK:

```
ground_Speed = "";
if(ground_speedString!=null){
	ground_Speed = ground_speedString;
}
else{
	Km_trackLength =  trackLength * 0.001;
	ground_speed = 0;

	if(hour > 0){
		ground_speed = Km_trackLength/hour;
	}
}
```

STRAIGHTNESS CALCULATION FOR THE LAST TRACK:

```
straightness = linear_distance/trackLength;
```

TORTUOSITY CALCULATION FOR THE LAST TRACK:

```
tortuosity = trackLength - linear_distance;
```

START A NEW TRACK PROCESS

```
        firstX = nextPoint.x;
        firstY = nextPoint.y;
        starTime =nextPoint.hour;
        timeTrackLength = nextPoint.hour;
        hasFirstPoint = true;
        hasFirstTimeTrackLength = false;
        last_index = nextPoint.index;
        radarDistance = "";
        Radardistance = distance(0, 0, nextPoint.x, nextPoint.y);
        if(Radardistance >0){
                radarDistanceString += radarDistance +"|";
        }
}
if(!hasLastPoint){
        lastX = nextPoint.x;
        lastY = nextPoint.y;
        endTime = nextPoint.hour;
}
start = false;
checkPoint = false;
}
```

2) <u>For the parameters calculated in vertical mode:</u>

CASE 1: EARTH PROFILE IS A SET OF GEOLOCALIZED POINT

```
for(Point nextPoint :listPoint):

        firstX = secondX;
        firstY = secondY;
        secondX = nextPoint.x;
        secondY = nextPoint.y;

        X = X_input/PixelToM_scale;

        Y = Y_input/PixelToM_scale;

        Point p = intersection(X,Y,X,0,firstX,firstY,secondX,secondY);

        CASE A: INTERSECTION POINT IS FOUND

        quotaMare  =  Y + Radar.centerY;
        quotaSuolo = quotaMare - (p.y * PixelToM_scale));

        break;

        CASE B: INTERSECTION POINT ISN'T FOUND - IT CALCULATES DISTANCE FROM INPUT
```

POINT TO X_AXIS

quotaMare = Y + Radar.centerY;

quotaSuolo = quotaMare - (Radar.y * PixelToM_scale);

CASE 2: EARTH PROFILE IS THE X-AXES

quotaMare = Y + Radar.centerY;

quotaSuolo = quotaMare - (Radar.y * PixelToM_scale);

SM3. Simplified example of the output of *Hypatia-trackRadar*. For visualization purposes, we included only the first echo of each track and we omitted some of the columns originally in the table. Field names were modified to improve readability. The track id (column "track_id") and the associated information correspond to the tracks shown in Fig. 5.

track_id	season	timestamp	X_utm	Y_utm	species 1	species 2	flock type	flock size 1	flock size 2	duratio n	soar	glide	length	ground speed	cross-country speed	straight	tort
K_a	spring	22/03/2016 10:38	570220	4232826	Black kite		flock	2		88	32	56	1,327.240	19.0717	13.860	0.920	107.550
BS_a	spring	29/04/2016 18:55	569508	4231067	Black stork		flock	2		140	0	140	1,920.430	13.7174	9.630	0.700	572.240
E_a	spring	26/04/2016 17:17	568836	4231755	Boot. eagle		single	1		119	29	90	1,460.640	8.1948| 17.0771	11.519	0.940	898.980
CB_a	spring	29/03/2016 14:48	569223	4232181	Com. buzzard		single	1		96	9	87	1,150.090	13.2951| 12.0816	11.342	0.950	612.480
CB_b	spring	27/04/2016 15:11	569108	4231942	Com. buzzard		single	1		100	38	62	1,149	13.7454| 15.9834	11.212	0.980	278.530
FT_a	spring	22/03/2016 11:25	569803	4232482	Com. kestrel		single	1		143	48	95	1,382.140	7.1387| 12.1544	5.486	0.570	597.620
HB_a	spring	21/04/2016 13:24	569062	4232537	Hon. buzzard		flock	3		202	85	117	2,701.570	6.282| 10.9071	5.740	0.430	1,542.070
HB_b	spring	29/04/2016 11:17	568841	4232592	Hon. buzzard		flock	3		26	0	26	2,601.010	10.0039	9.198	0.920	209.620
HB_c	spring	05/05/2016 14:05	568478	4231314	Hon. buzzard		flock	5		209	8	201	2,138.250	9.2525| 10.8386	10.052	0.980	374.240
HB_d	spring	05/05/2016 13:29	568708	4231302	Hon. buzzard		flock	2		268	54	214	2,079.750	6.379| 9.2254| 10.4933	7.153	0.920	162.730
HB_e	spring	05/05/2016 13:52	568738	4230936	Hon. buzzard		flock	11		315	114	201	2,059.670	13.9595| 8.0504| 7.3913	5.572	0.850	304.500
HB_f	spring	05/05/2016 14:54	568835	4231246	Hon. buzzard		flock	16		205	44	161	1,967.090	10.7946	7.831	0.820	361.720
MH_a	spring	27/03/2016 16:03	569094	4231059	Marsh harrier		single	1		164	48	116	1,905.390	12.6801| 14.5647	10.966	0.940	106.890
MH_b	spring	28/03/2016 18:37	569730	4231119	Marsh harrier		flock	3		157	0	157	1,736.320	11.0594	10.608	0.960	707.900

<table>
<tr><td>SE_a</td><td>spring</td><td>05/05/2016 15:00</td><td>568959</td><td>4232002</td><td>Snake eagle</td><td>single</td><td>1</td><td>233</td><td>67</td><td>166</td><td>2,287.330</td><td>12.6549|
8.4211|
12.9199</td><td>7.045</td><td>0.720</td><td>645.790</td></tr>
<tr><td>WS_a</td><td>spring</td><td>30/03/2016 16:17</td><td>568109</td><td>4231042</td><td>White stork</td><td>flock</td><td>24</td><td>184</td><td>0</td><td>184</td><td>2,825.560</td><td>15.3563</td><td>14.456</td><td>0.940</td><td>165.740</td></tr>
<tr><td>BE_1</td><td>autumn</td><td>07/09/2016 13:10</td><td>570916</td><td>4229833</td><td>Bee eater</td><td>flock</td><td>25</td><td>275</td><td>0</td><td>275</td><td>3,494.030</td><td>12.7056</td><td>9.726</td><td>0.770</td><td>819.460</td></tr>
<tr><td>BE_2</td><td>autumn</td><td>02/09/2016 18:15</td><td>572996</td><td>4228566</td><td>Bee eater</td><td>flock</td><td>27</td><td>141</td><td>0</td><td>141</td><td>1,557.270</td><td>11.0445</td><td>10.437</td><td>0.940</td><td>856.590</td></tr>
<tr><td>BE_3</td><td>autumn</td><td>02/09/2016 14:17</td><td>572129</td><td>4228699</td><td>Bee eater</td><td>flock</td><td>25</td><td>207</td><td>97</td><td>110</td><td>1,536.460</td><td>9.1533|
8.9534|
14.8329</td><td>6.205</td><td>0.840</td><td>251.970</td></tr>
<tr><td>BE_4</td><td>autumn</td><td>04/09/2016 11:00</td><td>571496</td><td>4229453</td><td>Bee eater</td><td>flock</td><td>23</td><td>122</td><td>0</td><td>122</td><td>1,439.340</td><td>11.7979</td><td>10.168</td><td>0.860</td><td>198.830</td></tr>
<tr><td>BE_5</td><td>autumn</td><td>25/08/2016 11:02</td><td>572242</td><td>4228666</td><td>Bee eater</td><td>flock</td><td>40</td><td>170</td><td>54</td><td>116</td><td>1,347.290</td><td>5.2275|
10.8162</td><td>6.739</td><td>0.850</td><td>201.620</td></tr>
<tr><td>BE_6</td><td>autumn</td><td>26/08/2016 13:30</td><td>571302</td><td>4228866</td><td>Bee eater</td><td>flock</td><td>20</td><td>62</td><td>0</td><td>62</td><td>1,095.840</td><td>17.6748</td><td>16.832</td><td>0.950</td><td>522.720</td></tr>
<tr><td>K_1</td><td>autumn</td><td>13/08/2016 09:55</td><td>571222</td><td>4229880</td><td>Black kite</td><td>flock</td><td>30</td><td>341</td><td>133</td><td>208</td><td>3,397.240</td><td>10.8978|
13.934</td><td>8.245</td><td>0.830</td><td>585.680</td></tr>
<tr><td>K_2</td><td>autumn</td><td>22/08/2016 16:36</td><td>571903</td><td>4229059</td><td>Black kite</td><td>flock</td><td>27</td><td>140</td><td>0</td><td>140</td><td>1,831.770</td><td>13.0841</td><td>12.675</td><td>0.970</td><td>572.060</td></tr>
<tr><td>K_3</td><td>autumn</td><td>16/08/2016 12:25</td><td>572082</td><td>4228746</td><td>Black kite</td><td>flock</td><td>12</td><td>165</td><td>0</td><td>165</td><td>1,692.490</td><td>10.2576</td><td>9.848</td><td>0.960</td><td>673.680</td></tr>
<tr><td>K_4</td><td>autumn</td><td>11/09/2016 12:08</td><td>572389</td><td>4228819</td><td>Black kite</td><td>flock</td><td>25</td><td>87</td><td>0</td><td>87</td><td>1,078.450</td><td>12.3961</td><td>12.177</td><td>0.980</td><td>190.590</td></tr>
<tr><td>CB_1</td><td>autumn</td><td>25/08/2016 10:38</td><td>571669</td><td>4228639</td><td>Com. buzzard</td><td>flock</td><td>1</td><td>100</td><td>1</td><td>99</td><td>1,033.490</td><td>5.2974|
10.3581</td><td>9.359</td><td>0.910</td><td>975.730</td></tr>
<tr><td>HB_1</td><td>autumn</td><td>24/08/2016 13:41</td><td>570976</td><td>4229800</td><td>Hon. buzzard</td><td>flock</td><td>16</td><td>201</td><td>10</td><td>191</td><td>2,592.500</td><td>15.843|
7.9623</td><td>12.528</td><td>0.970</td><td>742.800</td></tr>
<tr><td>HB_10</td><td>autumn</td><td>11/09/2016 13:11</td><td>571202</td><td>4229793</td><td>Hon. buzzard</td><td>single</td><td>1</td><td>123</td><td>0</td><td>123</td><td>1,310.480</td><td>10.6544</td><td>10.174</td><td>0.950</td><td>590.720</td></tr>
<tr><td>HB_11</td><td>autumn</td><td>26/08/2016 12:51</td><td>571689</td><td>4228599</td><td>Hon. buzzard</td><td>flock</td><td>5</td><td>91</td><td>0</td><td>91</td><td>1,014.220</td><td>11.1454</td><td>10.517</td><td>0.940</td><td>571.500</td></tr>
<tr><td>HB_2</td><td>autumn</td><td>24/08/2016 13:25</td><td>570869</td><td>4229059</td><td>Hon. buzzard</td><td>flock</td><td>30</td><td>215</td><td>0</td><td>215</td><td>2,114.890</td><td>9.8367</td><td>8.940</td><td>0.910</td><td>192.870</td></tr>
<tr><td>HB_3</td><td>autumn</td><td>24/08/2016</td><td>571649</td><td>4228799</td><td>Hon.</td><td>flock</td><td>33</td><td>210</td><td>68</td><td>142</td><td>1,922.400</td><td>5.6993|</td><td>8.005</td><td>0.870</td><td>241.290</td></tr>
</table>

		13:26			buzzard									13.4993			
HB_4	autumn	26/08/2016 11:05	573783	4229866	Hon. buzzard		flock	85		166	4	162	1,884.820	13.1747| 10.0389	10.165	0.900	197.500
HB_5	autumn	26/08/2016 10:44	572242	4228619	Hon. buzzard		flock	59		271	107	164	1,868.790	8.0415| 9.4098| 4.3617	5.302	0.770	431.920
HB_6	autumn	26/08/2016 11:12	573062	4229926	Hon. buzzard		flock	39		175	80	95	1,803.300	14.0377| 10.9489	9.197	0.890	193.850
HB_7	autumn	24/08/2016 13:23	570769	4228706	Hon. buzzard		flock	50		149	0	149	1,738.740	11.6694	11.034	0.950	946.420
HB_8	autumn	26/08/2016 12:01	570735	4228899	Hon. buzzard		flock	12		101	16	85	1,473.560	16.3635	14.302	0.980	290.690
HB_9	autumn	07/09/2016 10:09	571162	4229833	Hon. buzzard		single	1		148	2	146	1,429.700	9.5615	7.921	0.820	257.340
MF_1	autumn	13/09/2016 15:19	571549	4228999	Hon. buzzard	Marsh harrier	mixed flock	5	1	106	0	106	1,129.680	10.6574	10.164	0.950	522.930
MF_2	autumn	14/09/2016 11:41	571322	4229840	Hon. buzzard	Marsh harrier	mixed flock	5	1	84	0	84	1,012.690	12.0559	11.740	0.970	265.110
MH_1	autumn	14/09/2016 10:13	571523	4229013	Marsh harrier		flock	3		107	1	106	1,129.260	10.3987	9.566	0.910	105.660
MH_2	autumn	10/09/2016 10:30	571209	4228973	Marsh harrier		single	1		82	0	82	1,101.090	13.4279	13.250	0.990	145.520
WS_1	autumn	26/08/2016 11:51	574083	4229753	White stork		flock	33		318	150	168	3,078.140	11.004| 6.1711| 20.2459	8.612	0.890	339.380
WS_2	autumn	03/09/2016 14:35	570842	4229580	White stork		flock	6		319	26	293	2,101.280	8.0758| 8.5494| 2.9327| 7.1363| 6.8319	3.069	0.470	1,122.130